The near neutrino detector for the T2K experiment

Yury Kudenko[*]

Institute for Nuclear Research RAS
60 October Revolution Pr. 7A, 117312 Moscow, Russia

Representing the T2K Collaboration

Abstract

The T2K experiment is a second generation long baseline neutrino oscillation experiment designed as a sensitive search for ν_e appearance. The T2K near neutrino detector complex is located 280 meters from the pion production target and will measure both neutrino beam properties close to the production point and interaction cross sections. The main design features, test results and status of these detectors are presented.

1 Introduction

In recent years, the atmospheric [1], solar [2], reactor [3], and accelerator [4,5] experiments have provided convincing evidence of neutrino oscillations and therefore have demonstrated that neutrinos have non–zero masses. This phenomenon is the first clear example of new physics beyond the Standard Model which assumes neutrinos are massless particles. Three generation neutrino oscillations are described by six independent parameters: three mixing angles $\sin^2\theta_{12}, \sin^2\theta_{23}, \sin^2\theta_{13}$, two mass-squared differences $\Delta m_{21}^2 = m_2^2 - m_1^2$ and $\Delta m_{23}^2 = m_3^2 - m_2^2$, and one complex phase δ. Both mass differences and two mixing angles (θ_{12} and θ_{23}) are measured. The mixing angle θ_{13} was found to be small and only an upper limit was obtained [6, 7]. Presently nothing is known about the CP violating Dirac phase δ. The near–future neutrino oscillation experiments will be focused on the measurements of the unknown neutrino parameters: θ_{13}, mass hierarchy, and δ. Another important goal of these experiments is to measure the known mixing parameters more precisely.

---

[*]*Email address:* kudenko@inr.ru

2 Principles of T2K

The T2K (Tokai–to–Kamioka) experiment [8] will use a high intensity off–axis neutrino beam generated by a 50 GeV (initially 30 GeV) proton beam at JPARC (Japan Proton Accelerator Research Complex), SuperKamiokande as a far neutrino detector, and a set of dedicated neutrino detectors located at a distance of 280 m from the pion production target to measure the properties of the unoscillated neutrino beam. The schematic view of the T2K setup is shown in Fig. 1. The first phase of T2K has two main goals: a sensitive
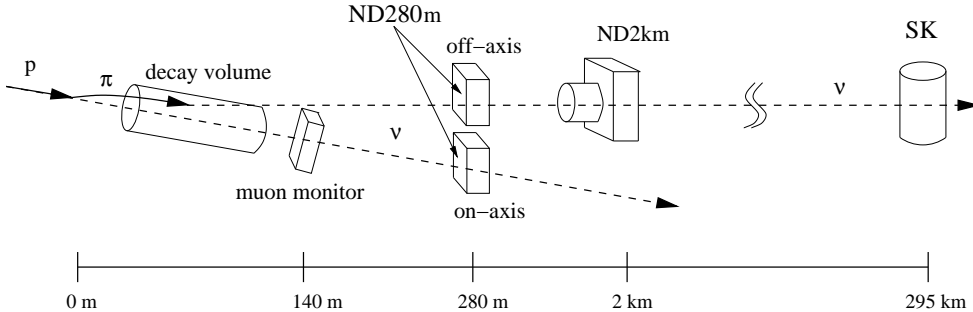

Figure 1: General layout of the T2K experiment. The basic elements are the neutrino beam line, muon monitor, near neutrino detector at 280 meters from the pion production target, and the far neutrino detector SuperKamiokande. Possible future 2km near detector is also shown.

measurement of θ_{13} and a more accurate determination of the parameters $\sin^2 2\theta_{23}$ and Δm_{23}^2 than any previous experiment.

The probability of ν_μ transition to ν_e can be approximately given by

$$P(\nu_\mu \rightarrow \nu_e) \approx 4\cos^2\theta_{13}\sin^2\theta_{13}\sin^2\theta_{23}\sin^2\left(\frac{1.27\Delta m_{13}^2(\text{eV}^2)L(\text{km})}{E_\nu(\text{GeV})}\right), \tag{1}$$

where L is the ν flight distance, and E_ν is the neutrino energy. It follows from this expression, the maximum sensitivity to the $\nu_\mu \rightarrow \nu_e$ transition is expected around the oscillation maximum for $\Delta m_{13} \simeq \Delta m_{23} = \Delta m_{atm} \simeq 2.5 \times 10^{-3}$. Based on this value, the neutrino peak energy in T2K should be tuned to ≤ 1 GeV to maximize the sensitivity for muon neutrino oscillations for a baseline of 295 km.

T2K will adopt an off–axis beam configuration in which neutrino energy is almost independent of pion energy and quasi-monochromatic neutrino spectrum can be achieved. The neutrino beam is produced from pion decays in a 94 m decay tunnel filled with 1 atm He gas at an angle of 2.5° with respect to the proton beam axis, providing a narrow neutrino spectrum with mean neutrino energies from 0.7 to 0.9 GeV, as shown in Fig. 2. The high energy tail is considerably reduced at 2.5° in comparison with the standard on-axis wide-band beam. This minimizes the neutral current π^0 background in the ν_e
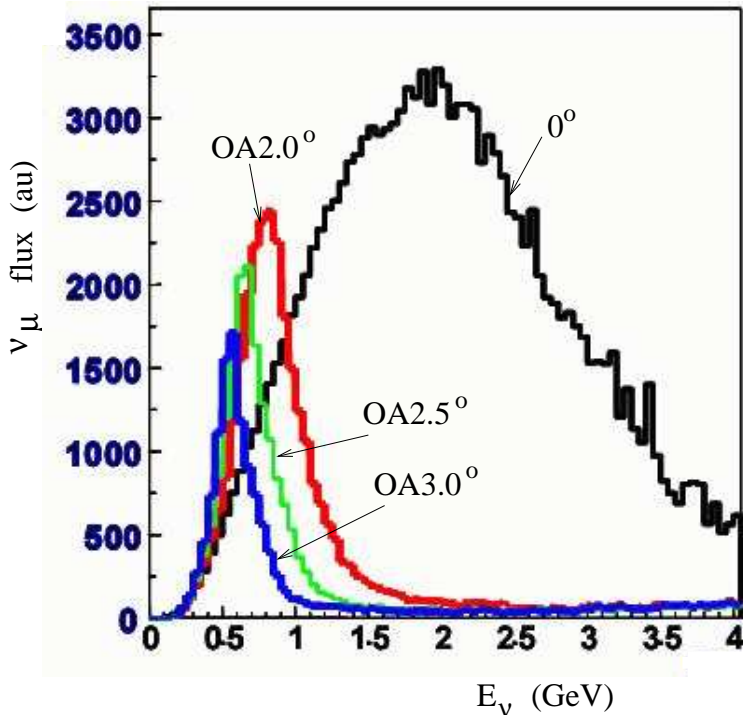
Figure 2: Neutrino energy spectra at 0° and different off-axis angles.

appearance search. Moreover, the intrinsic contamination of ν_e's from muon and kaon decays is expected to be about 0.4% around the peak energy.

To achieve T2K goals, precise measurements of the neutrino flux, spectrum and interaction cross sections are needed. For these purposes, the near detector complex (ND280) [9] will be built at a distance of 280 m from the target along the line defined by the average pion decay point and SK (see Fig. 1). This complex has two detectors: an on-axis detector (neutrino beam monitor) and an off–axis detector. Physics requirements for ND280 can be briefly summarized as follows: the absolute energy scale of the neutrino spectrum must be calibrated with 2% precision, and the neutrino flux monitored with better than 5% accuracy. The momentum resolution of muons from the charged current quasi-elastic interactions (CCQE) should be less than 10%, and the threshold for detection of recoil protons is required to be about 200 MeV/c. The ν_e fraction should be measured with an uncertainty of $\leq 10\%$. A measurement of the neutrino beam direction, with a precision much better than 1 mrad, is required from the on-axis detector.

3   Near neutrino detectors

3.1   On-axis neutrino monitor

The role of the on-axis neutrino detector (INGRID) is to monitor the neutrino beam direction and profile on a day to day basis. It consists of $7+7$ identical modules, arranged

to form a cross-configuration, and 2 diagonal modules, as shown in Fig. 3. INGRID
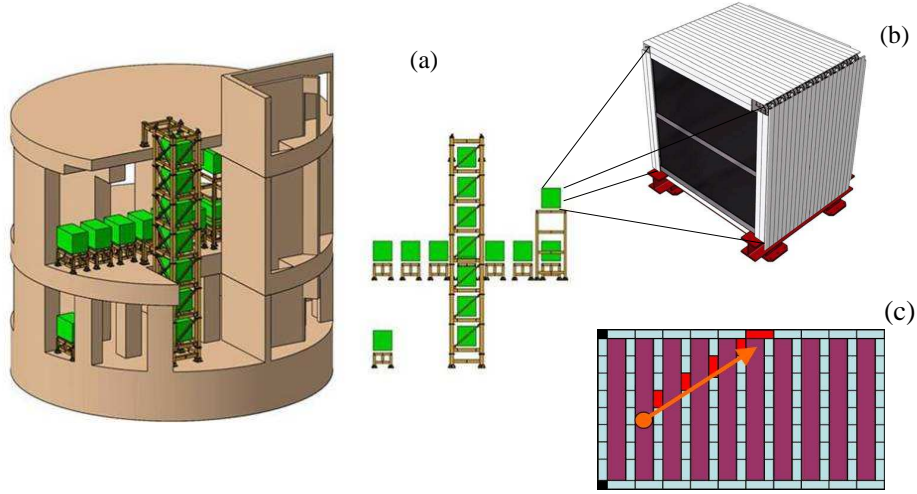

Figure 3: (a) schematic view of INGRID; (b) segmented iron-scintillator sandwich module; (c) a charged current neutrino interaction with muon track.

samples the neutrino beam profile with an area of 9×9 m^2. Each iron-scintillator sandwich module covers an area of 125×125 cm^2 and weighs 10 tons. The module consists of ten 6.5 cm-thick iron layers and 11 scintillator tracking planes, and is surrounded by four veto counters. Each tracking plane has one vertical and one horizontal scintillator layer composed of $5 \times 1 \times 121$ cm^3 scintillator slabs. Each scintillator has a central hole to insert a wavelength shifting (WLS) fiber for light collection and routing to a photosensor. The total mass of INGRID is ~ 160 tons. A typical event rate detected by the center module every spill is expected to be about 0.5 per ton, i.e. the whole INGRID will detect more than 10^5 neutrino events/day. In order to minimize the systematic from the uncertainty of the off-axis angle, the neutrino beam direction will be monitored by INGRID with a precision of $<< 1$ mrad each day at designed intensity.

3.2 Off-axis near detector

The off-axis detector (Fig. 4) includes the UA1 magnet operating with a magnetic field of 0.2 T, a Pi-Zero detector (POD), a tracking detector which includes time projection chambers (TPC's) and fine grained scintillator detectors (FGD's), an electromagnetic calorimeter (Ecal), and a side muon range detector (SMRD).

3.2.1 Photosensors

Wavelength shifting fibers will be widely used for readout of all scintillator detectors which are the main active element of the ND280 detector. A magnetic field environment and
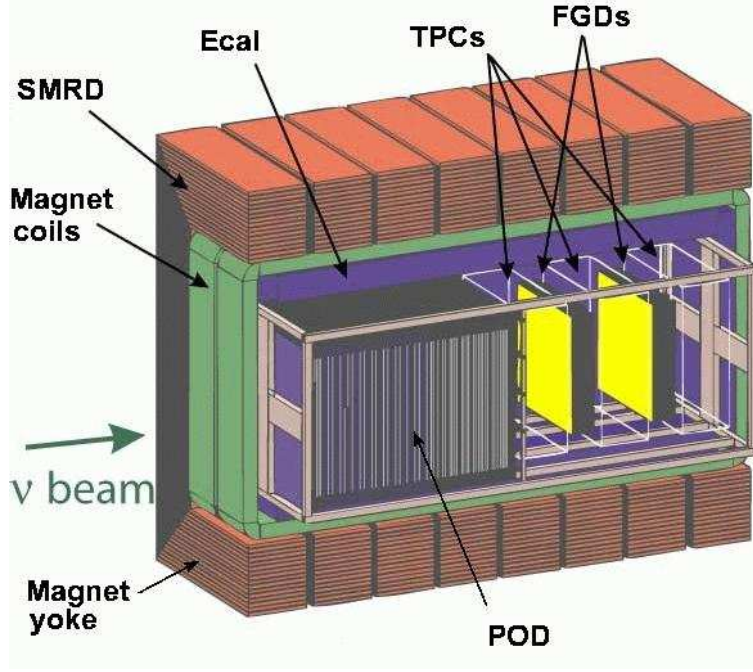
Figure 4: The cutaway view of the T2K near detector.

limited space inside the UA1 magnet put serious constraints for the usage of standard photodetectors such as traditional multi-anode photomultipliers. Since the ND280 has about 60k individual readout channels, the cost of photosensors is also very important. After studying several candidates, a multi-pixel avalanche photo-diode operating in the limited Geiger multiplication mode was selected as the baseline detector. These novel devices are compact, well matched to spectral emission of WLS fibers, and insensitive to magnetic fields [10–12]. The required parameters for these photosensors from all ND280 subdetectors can be summarized as follows: an active area diameter of ~ 1 mm, photon detection efficiency for green light $\geq 20\%$, pixels number > 400, and a dark rate at operating conditions ≤ 1 MHz. The gain should be $(0.5 - 1.0) \times 10^6$, the cross−talk $\sim 10\%$, and pulse width should be less than 100 ns to meet the spill structure of the JPARC proton beam. For calibration and control purposes, it is very desirable to obtain well separated single photoelectron peaks in amplitude spectra at operating temperature.

After a R&D study of 3 years, a Hamamatsu MPPC was chosen as the photosensor for ND280. The description of this device and its parameters can be found in Ref. [13]. The final T2K version is a 667 pixel MPPC with a sensitive area of 1.3×1.3 mm^2 (Fig. 5). These devices demonstrated good performance at room temperature: a low cross-talk value of about 10%, a photon detection efficiency for green light of $\geq 25\%$, a low dark rate of ~ 0.3 MHz at the operating voltage, a high gain of about 0.7×10^6, and a pulse width of less than 50 ns.
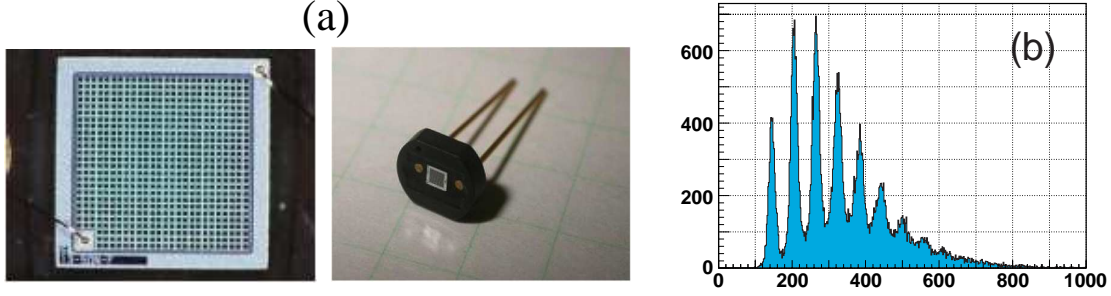
5

Figure 5: (a) The photograph of a 667 pixel MPPC: a magnified face view of an MPPC with a sensitive area of 1.3×1.3 mm^2 (left), the package of this MPPC (right); (b) ADC spectrum from an LED signal. Clearly separated peaks at equal intervals correspond to 0, 1, 2, 3... fired pixels.

3.2.2 POD

The POD is optimized for measurement of the inclusive π^0 production by ν_μ interactions on oxygen and will be installed in the upstream end of the magnet. The cross section measurements on an oxygen target will be achieved by using the following POD geometry: the upstream and downstream regions are configured as electromagnetic calorimeters providing energy containment and active veto, and the central region of the POD provides the fiducial mass for the π^0 measurements (Fig. 6(a)). The schematic view of a plane of the POD target is shown in Fig. 6(b). It consists of alternating water target layers of about 3 cm-thick and tracking layers composed of X-Y extruded triangular shaped scintillator bars of 17 mm in height and 32.5 mm at the base and a central hole for a WLS fiber. A thin sheet of brass (~ 1.6 mm-thick) is sandwiched in the 26 X-Y tracking layers of the target region. The upstream and downstream regions have 7 X-Y scintillator layers with 4 mm-thick lead radiators between them. The POD has a total mass of approximately 17 tons with a fiducial mass of about 3 tons of water and 8 tons of other materials. The tests of light yield of the POD scintillators with MPPC's connected to one end of a Y11 WLS fiber showed good results. The light yields for a minimum ionizing particles (MIP) are 19.8 p.e./MeV and 8.7 p.e./MeV at 25 and 205 cm from the MPPC, respectively. With the mirrored far end of the WLS fiber, the light yield of 15.7 p.e./MeV is much greater than the 5 p.e./MeV required for efficient reconstruction of electromagnetic showers.

Oxygen cross section measurements will be made by comparing the interaction rate of events collected with water in the target region versus similar running periods with water removed from the target region. A typical neutral current event with a π^0 is shown in Fig. 6(c) in which a neutral pion is accompanied by a neutron. The energy resolution for events fully contained in the active target is expected to be about $10\% + 3.5\%/\sqrt{\text{GeV}}$ and the reconstruction efficiency of a π^0 with a momentum ≥ 200 MeV/c is expected to be approximately 33%.
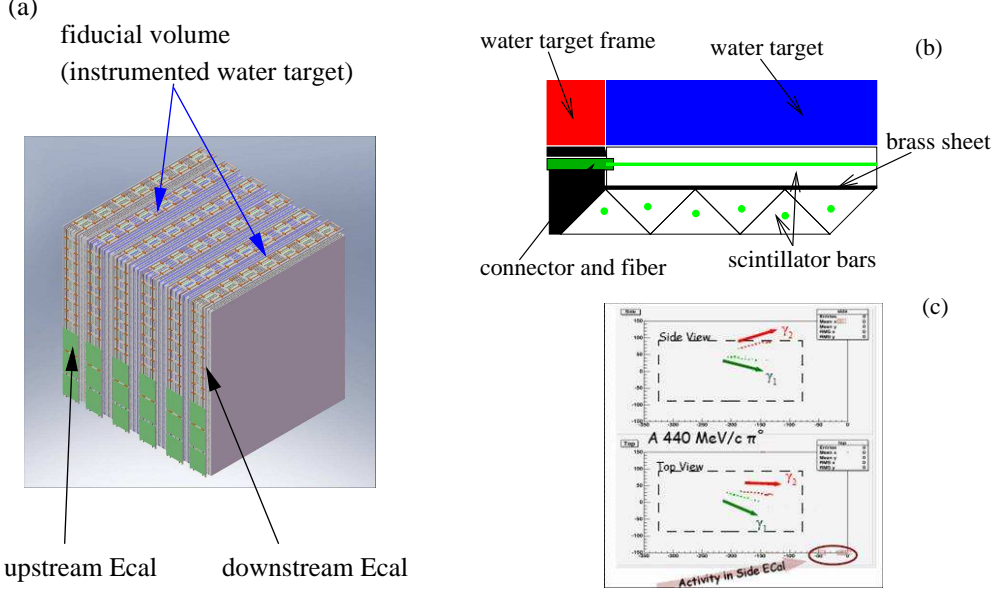
Figure 6: (a) POD schematic view: the central region is constructed of alternating water target and scintillator tracking layers; (b) one layer of the target region; (c) a neutral current π^0 event in POD. The horizontal and vertical axes are in centimeters.

3.2.3 ND280 tracker

The ND280 tracker consists of three TPC's and two FGD's, as shown in Fig. 4. Its main function is to measure the muon and electron neutrino beam fluxes and energy spectra, plus various charged current cross sections. The tracker is designed to accurately measure CCQE events, the main process at the T2K peak neutrino energy,

$$\nu_\mu + n \rightarrow \mu^- + p. \tag{2}$$

In order to measure this process the reconstruction of both proton and muon is useful. The proton will be primarily identified and measured by the FGD while the muon will be measured by the TPC. The initial neutrino energy will be reconstructed from the muon momentum. The measurements of CCQE events will be used for flux normalization in the oscillation analysis.

FGD. The ND280 will contain two FGD's, each with dimensions $1.84 \times 1.84 \times 0.3$ m^3 resulting in a total target mass of about 2.0 tons. The first FGD will be an active scintillator detector, similar to the SciBar detector [14] of the K2K experiment. It consists of thirty scintillator layers of 192 $0.96 \times 0.96 \times 184$ cm^3 extruded scintillator bars which are arranged in alternating vertical and horizontal layers perpendicular to the beam direction. The second FGD is composed of seven X-Y sandwiches of scintillator layers alternating with six 3-cm thick layers of water. The weight of the scintillator is 0.56 ton and of water,

0.44 ton. The readout of each scintillator bar is provided by an MPPC connected to one end of a WLS fiber inserted in a central hole. A beam test of scintillator bars performed at TRIUMF showed that the light yield for 120 MeV/c pions, muons, electrons will be more than 10 p.e. at the far end from a photosensor without mirroring the far end of the fiber. The mirroring increases the light yield by $\geq 80\%$, guaranteeing a detection efficiency of more than 99% for minimum ionizing particles. The FGD allows a clear separation between protons and pions using dE/dx information and tagging Michel electrons from the decay of short-ranged pions. Comparing the interaction rates in both FGD's permits separate measurement of neutrino cross sections on carbon and on water. About 4×10^5 neutrino interactions are expected in both FGD modules for a one year exposure with 10^{21} protons on target.

TPC. The primary purpose of the TPC is to measure the 3-momenta of muons produced in CCQE interactions in the FGD. The TPC will use a low diffusion gas to obtain the momentum resolution of $\leq 10\%$ for particles below 1 GeV/c. A 700 μm space point resolution per "row" of pads is required to achieve this momentum resolution. The absolute energy scale will be checked at the 2% level using the invariant mass of neutral kaons produced in DIS neutrino interactions and decaying in the TPC volume. A good dE/dx resolution of $< 10\%$ is expected for 72 cm long tracks which will provide better than 5σ separation between muon and electron tracks in the momenta range 0.3-1.0 GeV/c.

The three TPC modules are rectangular boxes with outer dimensions of approximately 2.5×2.5 m^2 in the plane perpendicular to the neutrino beam direction, and 0.9 m along the beam direction. A simplified drawing of the TPC is shown in Fig. 7. The TPC
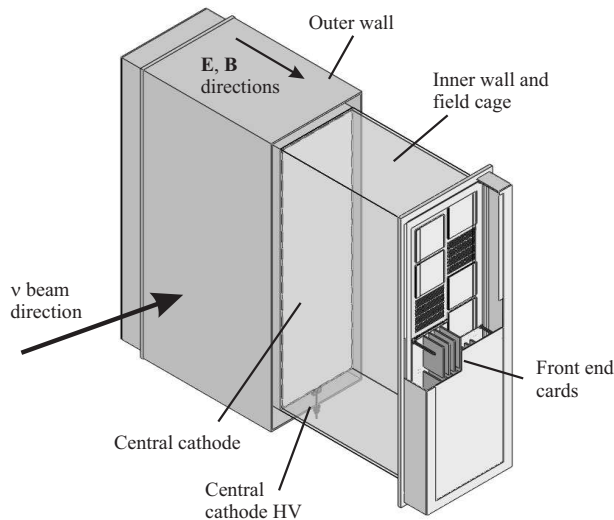

Figure 7: The layout of TPC showing the inner and outer boxes and the central cathode.

modules are operated at an electric field of 200 V/cm. The central cathode, which divides the drift space into two halves to limit the maximum drift distance to ~ 1 m, will be at a potential of -25 kV. The baseline gas choice is Ar(95%)–CF$_4$(3%)–iC$_4$H$_{10}$(2%).

8

The 'bulk' Micromegas detectors will be used to instrument the TPC readout plane. The active surface area of the Micromegas module is 359×342 mm^2 with 1726 active pads of 9.7×6.9 mm^2. 12 Micromegas modules will be used for each readout plane of the TPC. In total, the 3 TPC's will consist of 72 modules with ~ 124000 readout channels.

The first prototypes of Micromegas detectors have been tested with cosmic muons in the former HARP field cage setup with a magnetic field [15] and demonstrated good momentum resolution of 8.3% at 1 GeV/c. A dE/dx resolution of about 12% for track lengthes of about 40 cm and a good uniformity of $\sigma = 3.4\%$ for the gain ~ 1000 have been obtained.

A typical CCQE event for neutrino interaction in FGD1 is shown in Fig. 8. The
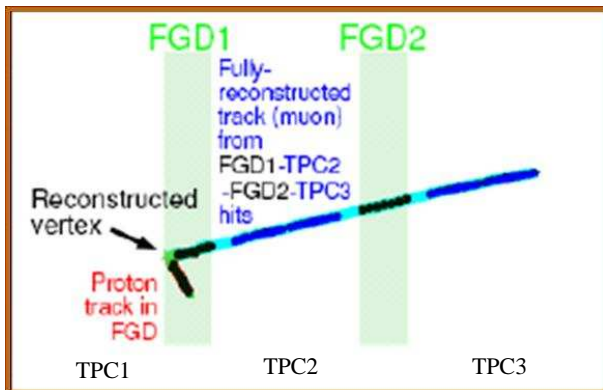

Figure 8: Typical CCQE event in the tracker.

reconstruction efficiency of CCQE events produced in the FGD with a track in the TPC is estimated to be about 50% at a $E_\nu \sim 0.7$ GeV.

3.2.4 Electromagnetic calorimeter

The Electromagnetic calorimeter (Ecal) shown in Fig. 9 consists of two sections. One surrounds the POD (POD Ecal) for detectioning photons and muons escaping the POD, and the second section, surrounding the FGD's and TPC's (TEcal), detects particles leaving the tracking volume.

TEcal modules are made of 4 cm-wide, 1 cm-thick plastic scintillator bars arranged in 32 layers and separated by 31 layers of 1.75 mm-thick lead sheets. The orientation of the bars alternates between layers so that the bars in any layer are perpendicular to the bars in the two adjacent ones. This bar width allows good π^0 reconstruction efficiency and provides the spatial resolution required for reconstruction of the direction of detected photons. The active length of the TEcal along the neutrino beam is 384 cm and the total depth is 50 cm corresponding to $10.5X_0$. TEcal has two side modules, one on each side of the UA1 iron yokes, one top and one bottom modules, each is split into two (left and right) so that they can move with the magnet yoke when the magnet opens. All
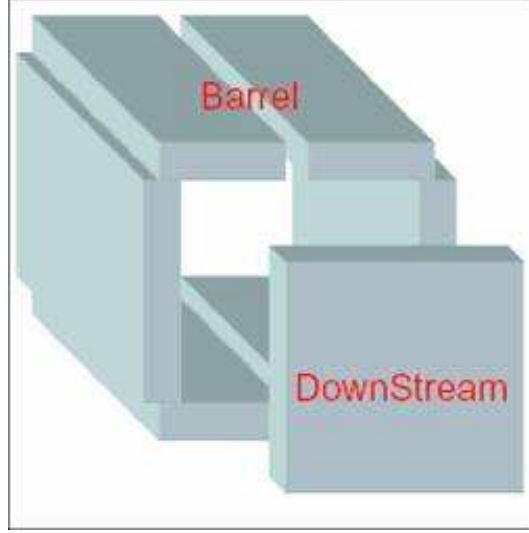
9

Figure 9: Basic structure of the electromagnetic calorimeter.

scintillator bars have a hole in the center with a 1 mm WLS fiber inserted in it. All long bars running along the neutrino beam are readout by an MPPC at each end (double-end readout), while all shorter bars (perpendicular to the neutrino beam) are mirrored at one end and readout by an MPPC at the other (single-end readout). The downstream Ecal is a single module with the same granularity as TEcal modules with an effective depth of $11X_0$. It is located at the downstream end of the magnet and covers an active surface area of 2×2 m^2. All bars have double-ended readout. The total weight of the TEcal and downstream Ecal is 28.3 tons.

The POD Ecal has modules with coarser segmentation and less total X_0 and does not provide good energy and spatial resolution required for π^0 reconstruction. These modules consist of 6 scintillator layers separated by 5 layers of 5 mm-thick lead converters resulting in an effective depth of $4.5X_0$.

The energy resolution of TEcal, dominated by sampling fluctuations, is estimated to be about $7.5\%/\sqrt{E(\text{GeV})}$ for energies up to 5 GeV. TEcal is expected to provide good electron/pion separation. An efficiency of 90% for electrons is expected with 95% pion rejection.

3.2.5   Side muon range detector

Muons which escape at large angles with respect to the neutrino beam can not be measured by the TPC's. However, they will intersect in the iron yoke and therefore a muon's momentum can be obtained from its range by instrumenting the iron at various depths. About 40% of muons from CCQE reactions and about 15% of muons from charge current non-quasi-elastic reactions are expected to enter the SMRD. In addition, the SMRD will be used to veto events from neutrino interactions in the magnet and in walls of the ND280 pit and will provide a cosmic trigger for calibration of inner detectors.

The UA1 iron yoke consists of 16 C-shaped elements made of sixteen 5 cm thick iron plates, with 1.7 cm air gap between the plates and is segmented in 12 azimuthal sections. The active component of the SMRD will consist of 0.7 cm thick scintillator slabs sandwiched between the iron plates of the magnet yokes. Details of the extrusion of the scintillator slabs and the method of etching the plastic surface by a chemical agent can be found in Ref. [16]. For the readout, we employ a single WLS fiber embedded in a serpentine shaped (S–shape) groove, as shown in Fig. 10. Such a shape allows the fiber
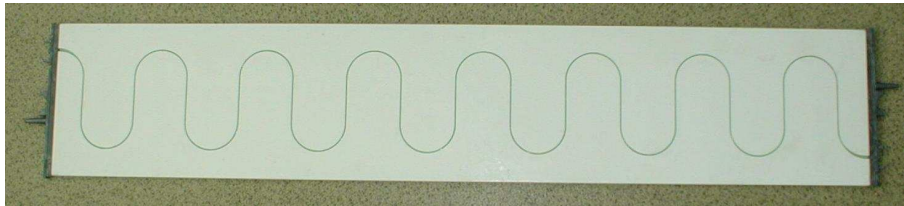

Figure 10: The SMRD counter with embedded Kuraray Y11 WLS fiber.

to collect the scintillation light over the whole surface of a scintillator slab [17]. Two MPPC's are coupled to both ends of a WLS fiber glued into the S–shape groove. The detector performance has been tested using cosmic muons. Typical ADC spectra for MIP's obtained with 1.0×1.0 mm^2 MPPC's are shown in Fig. 11. The SMRD counters tests resulted in a high detection efficiency measurement of greater than 99%, a time resolution of about 1 ns, and a spatial resolution along the slab of about 8 cm for minimum ionizing particles.

4 Conclusion

The T2K experiment has a rich physics potential and provides an excellent opportunity to greatly extend our understanding of neutrino properties. To achieve the physics goals of T2K, the complex of near neutrino detectors needed for measurement of the unoscillated neutrino beam properties is under construction. The on-axis detector will be ready to accept the first neutrino beam in April 2009, the installation and commissioning of the whole off-axis detector will be finished during 2009. The T2K experiment is expected to start data taking in 2009.

References

[1] Y. Fukuda et al., (Super-Kamiokande Collaboration) Phys. Rev. Lett. 81 (1998) 1562.
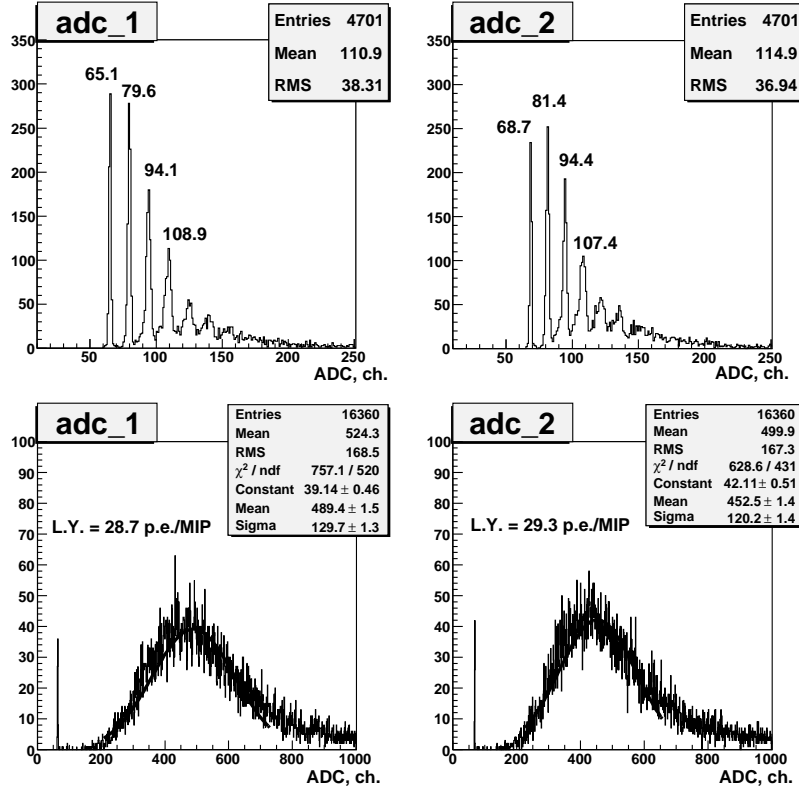
Figure 11: The ADC spectra of the SMRD counter for minimum ionizing particles measured at 22°C. The light yield (sum of both ends) is equal to 58 p.e.

[2] Q.R. Ahmad et al., (SNO Collaboration) Phys. Rev. Lett. 87 (2001) 071301; Q.R. Ahmad et al., (SNO Collaboration) Phys. Rev. Lett. 89 (2002) 011301.

[3] K. Eguchi et al., (KamLAND Collaboration) Phys. Rev. Lett. 90 (2003) 021802.

[4] M.H. Ahn et al., (K2K Collaboration) Phys. Rev. D74 (2006) 072003; E. Aliu et al., (K2K Collaboration) Phys. Rev. Lett. 94 (2005) 081802.

[5] D.G. Michael et al., (MINOS Collaboration) Phys. Rev. Lett. 97 (2006) 191801.

[6] M. Apollonio et al., (CHOOZ Collaboration) Eur. Phys.J. C27 (2003) 331.

[7] S. Yamamoto et al., (K2K Collaboration) Phys. Rev. Lett. 96 (2006) 181801.

[8] Y. Itow et al., hep-ex/0106019.

[9] "T2K ND280 Conceptual Design Report", T2K Internal Document. See also D. Karlen, Nucl. Phys. B (Proc. Suppl.) 159 (2006) 91.

[10] G. Bondarenko et al., Nucl. Instr. Meth. A442 (2000) 187.

[11] P. Buzhan et al., Nucl. Instr. Meth. A504 (2003) 48.

[12] V. Andreev et al., Nucl. Instr. Meth. A540 (2005) 368; D. Beznosko et al., FERMILAB-PUB-05-410.

[13] Hamamatsu Photonics K. K., http://www.hamamatsu.com; M. Yokoyama et al., arXiv:physics/0605241; S. Gomi et al., Nucl. Instr. Meth. A581 (2007) 427.

[14] K. Nitta et al., Nucl. Instr. Meth. A535 (2004) 147; S. Yamamoto et al., IEEE Trans. Nucl. Sci. 52 (2005) 2992.

[15] J. Bouchez et al., Nucl. Instr. Meth. A574 (2007) 425.

[16] Yu.G. Kudenko et al., Nucl. Instr. Meth. A469 (2001) 340; O. Mineev et al., Nucl. Instr. Meth. A494 (2002) 362; N. Yershov et al., Nucl. Instr. Meth. A543 (2005) 454.

[17] O. Mineev et al., Nucl. Instr. Meth. A577 (2007) 540.